

Thermoluminescence, glow curves and carrier traps in colored and nominally pure LiF crystals

© G. Baldacchini, P. Chiacchiaretta, V. Gupta*, V. Kalinov**, A.P. Voitovich**

ENEA, Frascati Research Center, Department of Physical Technologies and New Materials, 00044 Frascati, Roma, Italy

* Department of Materials & Metallurgical Engineering, Indian Institute of Technology-Kanpur, 208016 Kanpur, Uttar Pradesh, India

** Institute of Physics, Academy of Sciences of Belarus, 220072 Minsk, Belarus

E-mail: baldacchini@frascati.enea.it

Thermoluminescence (TL) of nominally pure LiF crystals irradiated with gamma rays has been studied in connection with color centers (CCs) generated during ionizing irradiation. A close analysis of the experimental TL spectra has unveiled the existence of 10 glow peaks (GPs) spanning from 100 to 450°C. The relatively well resolved GPs up to 263°C have been associated to F_3^+ , F_3 and F_2 CCs, while the remaining tangled ones have been attributed to F and F -like CCs. A first order kinetics approach has been used to simulate the TL spectra, and the appropriate parameters of the carrier traps have been obtained. A critical analysis of their values has shown on one side the usefulness of using pure crystals to understand their basic contributions to TL, and on the other side the possible existence of further weak GPs and the role still played by the residual amount of impurities.

V.S. Kalinov is grateful to ENEA for a fellowship allowing him the carrying out of part of this work in Frascati.

PACS: 78.60.Kn, 61.72.Ji, 81.40.Ef, 78.40.Ha

1. Introduction

The picture of the nature of thermoluminescence (TL) in insulating crystals is still slightly blurred. Although it is known that irradiated samples of crystalline alkali halides, for instance, release luminous energy when heated above the irradiation temperature, the inner mechanisms of the phenomenon are still debated. This is mostly due to the large number of the processes involved. Physical models of TL have been proposed by various authors [1–3]. The general scheme admits a discrete number of localized levels in the forbidden energy gap between the valence and conduction bands. Several levels below the bottom of the conduction band serve as electron traps, and by analogy several trapping levels for positive holes are assumed to be present above the valence band. Heating the sample causes the trapped electrons from one level to move in the empty conduction band from where they decay toward the valence band, releasing energy often in form of light. A single glow peak (GP) is so generated during the heating process. If more than one trapping level exists in the band gap, multiple GPs are produced and the total TL curve may be difficult to be interpreted. Moreover, it is obvious that the trapping levels and the relative GPs are strictly related to the color centers (CCs) produced by the ionizing radiation and the impurities, which are often inserted on purpose in the crystals. The complex and tangled mechanisms and the many actors involved make it almost impossible to understand the details of TL processes.

However, TL is expected to be very much simplified in case impurities are absent or reduced to a bearable minimum. Studies in the previous direction have been started recently in γ -colored LiF [4–7], which is one of

the most common material among alkali halides for its peculiar optical properties [8,9], and is also popular as a solid dosimeter for ionizing radiation [10]. By measuring TL curves of four LiF crystals, which have been optically characterized before the heating procedures, and by using also the results of annealing measurements on similar crystals, it has been possible to associate a few GPs to well defined and known CCs, an important step on the way to clarify the TL hidden mechanisms. However, not all GPs have been linked to defect centers, and not all of them have been yet discovered and described appropriately.

It is the purpose of this work a close study of the total TL curve, the finding of all the GPs involved, and their analysis to retrieve the energy parameters related to the carrier traps, and hopefully to the CCs already associated to some GPs. For this aim, the present report will be organized as in the following. In chapter 2 the results obtained recently on the matter under discussion will be briefly reviewed, in chapter 3 the work done here will be described in detail, and finally the conclusions will be drawn in chapter 4.

2. Experimental procedures, measurements and associations

2.1. Preparation of samples and optical properties. Cleaved and polished samples about 1 mm thick were taken from a bulk crystal of LiF containing less than 10 ppm of impurities. In particular, as far as the impurity ions are concerned, Ge is present at $2.3 \cdot 10^{-5}$ g/g (gram of impurity ion over gram of crystal material); Na at $1.8 \cdot 10^{-5}$, Fe at $0.9 \cdot 10^{-5}$, while other ions are at 10^{-6} or less, as it is the case for Mg at 10^{-9} . These samples were irradiated by the 1.17 MeV gamma rays of

Table 1. LiF samples, temperature of coloration with ^{60}Co , and temperature and optical treatments

Sample	Coloration	Treatment
A	RT with γ -rays	None
B	RT with γ -rays	Annealed at 200°C for 20 min
C	-60°C with γ -rays	None
D	-60°C with γ -rays	Pumped with 308 nm laser light at RT

Table 2. Energy parameters and peak intensity of absorption bands of the most prominent CCs in samples A, B, C, D as determined from transmission spectra measured at RT and their theoretical fit. The reported values of the linewidth ΔE refer to half width at half maximum (HWHM)

Color center	Band parameters			Intensity in sample, arb.units			
	λ_p , nm	E_p , eV	ΔE , eV	A	B	C	D
F	245	5.07	0.37	426	384	742	904
$F_3(R1)$	312	3.93	0.22	14	11	7	11
$F_3(R2)$	379	3.27	0.24	8	5	2	7
F_2	444	2.79	0.076	118	110	34	3
F_3^+	448	2.77	0.144	53	29	49	74
$F_4(N1)$	513	2.42	0.12	8	15	0.5	3
$F_4(N2)$	552	2.25	0.12	5	14	0.5	3

a ^{60}Co source with a dose rate of 0.7 kC/kg, and total dose 7 kGy ($0.85 \cdot 10^6$ R), which is a relatively low dose far from saturation and damage effects [3]. Two of them were irradiated at room temperature (RT) and the other two at -60°C. Of the samples colored at RT, one was left as such, sample A, while the other one was annealed at 200°C for about 20 min and then cooled quickly to RT, sample B. Of the samples colored at -60°C, one was left as such, sample C, while the other one was pumped at RT for about 1 h with the 308 nm line of a XeCl excimer laser, sample D. In this way, four different samples, A, B, C, D, were obtained, and the procedures of preparation are summarized in Table 1.

It is well known that irradiation of LiF by gamma rays, or by any other ionizing radiation, produces absorption bands all over the spectral region from 200 to 800 nm, due in the order of increasing wavelength and usually decreasing absorption intensity to F^- , F_3^- , F_2^- , F_3^{+} , F_4^- , F_2^+ -centers [8,11,12]. However, subsequent treatments with heat and laser light change the relative concentration of the remaining CCs. So, at the end of the preparation four samples with different amounts of F^- , F_3^- , F_2^- , F_3^{+} , and F_4^- -centers were at disposal for differentiated TL investigations. Indeed, it is expected that the same crystals, but with different concentrations of CCs, should produce different TL spectra, and in particular GPs with different intensity according to the amount and type of CCs.

The absorption spectra of the above prepared samples have been measured at RT by using a spectrophotometer Lambda 19DM Perkin-Elmer at a resolution of 1 nm. The exact amount of CCs in the samples has been determined by best fitting the optical transmission and emission bands with the sum of single Gaussian curves. For the optical transmission spectra, data reduction was performed according to a theoretical model that includes multiple reflections within the crystal and the effect of Gaussian absorption bands on the refractive index [13]. Besides the theoretical transmission curves, the fit procedure provides also the intensities of the absorption bands of the different types of CCs. They have been reported in Table 2, together with other important parameters of the involved CCs. Indeed, the values of the peak intensity of the absorption bands, in arbitrary units, are given with the wavelength λ_p and energy E_p of the peak of the same absorption bands, and also with their linewidth ΔE .

Moreover, in order to know better the relative concentration of those centers which are luminescent, mainly F_3^+ and F_2^- , also emission spectra were performed. In particular, photoluminescence was optically excited by the 458 nm line of an Ar ion laser, and revealed in a collinear geometry by using a Jobin Yvon Fluorolog-3 spectrofluorometer. The results obtained by studying the emission have confirmed and improved the previous ones obtained by transmission measurements.

2.2. Thermoluminescence and annealing measurements. TL measurements were performed in the range 40–500°C with a heating rate of 15°C/min. The apparatus and methods for measuring the TL curves have been reported elsewhere [14]. The TL curves from various crystals show considerable differences and the results from the four specimens are presented in Fig. 1. As expected from the previous different sample preparation methods, there are noticeable differences among the four crystals, which display different TL spectra. In order to observe better all the GPs, the TL curves of the samples have been positioned one on top of the other also in a logical sequence following the different treatments. In this way it has been possible to observe the existence of many common GPs which happen to be at about 164, 193, 228, 263, 286, 308, 332, and 410°C, as indicated by the vertical dotted lines in the same Fig. 1. Usually, GPs are not well visible in a complex TL spectrum, where only tips emerge on top of the spectrum, but usually these tips hint at the existence of full GPs underneath. However, it is also possible that some GPs go unnoticed because they are weak or too much tangled among other ones.

Besides the role of CCs in TL itself, we have discovered that also the fate of the single CC type in LiF as a function of temperature is not very well known, beyond some general recipes valid for all defect centers in alkali halides. For instance, the annealing process at certain temperatures eliminates in the order of complexity the aggregated CCs, and only F^- -centers remain at high temperatures. Usually, above 500°C also F^- -centers are destroyed and the crystal becomes

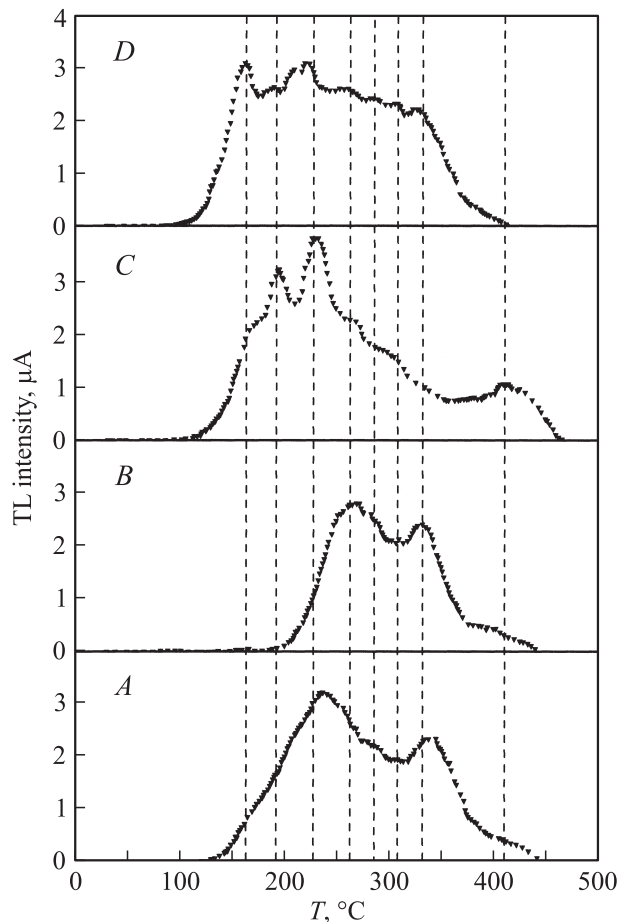


Figure 1. Experimental TL curves of the four samples A, B, C and D (dots) and positions of the eight GPs as determined visually (dashed vertical lines).

completely transparent, almost as before the irradiation processes with the exception of colloids formation below 300 nm.

However, while detailed annealing experiments, previously called bleaching because of the discoloration of the crystals, have been performed in ordinary alkali halides, like NaCl [15] and KCl [16], to our knowledge LiF has been studied only in a few cases and in a limited way [17,18]. For this reason, and in order to fill up the lacking of information on the subject, a systematic series of experiments have been performed to clarify the thermal annealing of previously colored LiF crystals [19].

A sample similar in dimensions and irradiation dose as the previous four ones has been utilized for the annealing measurements, and Fig. 2 shows its transmission spectrum with indicated the location of the main absorptions bands. The CCs reported in Fig. 2 are the only ones observed experimentally, and they are formed by aggregating two F -centers (F_2), three F -centers (F_3), four F -centers (F_4), and two F -centers and a vacancy (F_3^+). Complex CCs, like F_3 and F_4 , lay outside a single lattice plane, and can have different isomers which originate different absorption

bands. The F -center, which is the basic building block of all the other CCs, is formed by a single electron associated to a halide vacancy.

This crystal has been successively heated in an oven for 10 min at different temperatures from 50 to 550°C. After heating at each temperature, the sample was cooled quickly at RT, and its absorption spectrum measured thereafter. From all the previous spectra, the intensity values of the peak absorption for each CC have been derived with a precision of about 10%, and reported in Fig. 3 as a function of temperature in a log scale over more than three decades. Although the graph has been limited in the lower part, because of the minimum experimentally measurable absorption of $\sim 10^{-3}$ OD, the behavior of the various CCs is clearly enough displayed until their final demise. It is observed that CCs are bleached in the order of increasing temperatures as $F_3^+ \rightarrow F_4 \rightarrow F_3 \rightarrow F_2 \rightarrow F$, but during the

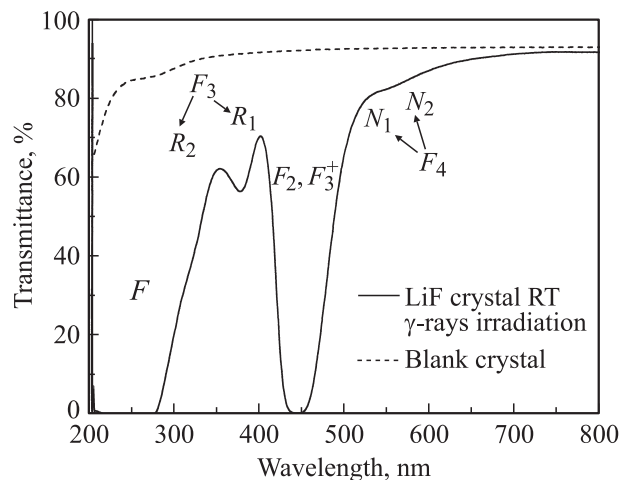


Figure 2. Transmission spectra at RT of a LiF crystal 2 mm thick colored at RT with γ -rays from a source of ^{60}Co at a dose of 10^7 R (solid line), and of a similar uncolored blank crystal (dashed line).

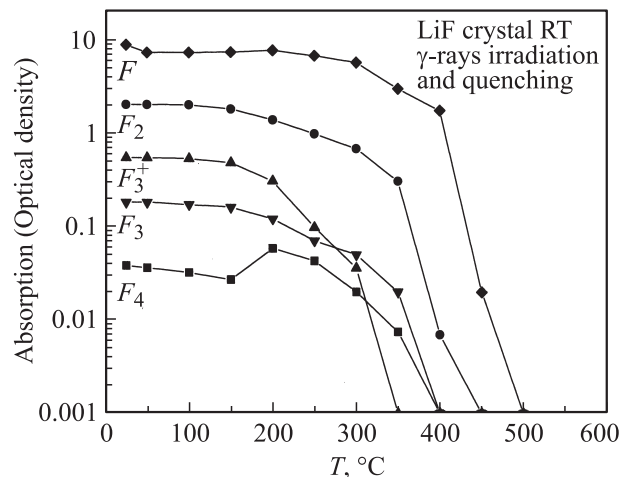


Figure 3. Absorption intensities of the CCs in the LiF crystal indicated in Fig. 2 as a function of the annealing temperature. As expected, the crystal is completely bleached above 500°C.

annealing from 200 to 300°C there are clear evidences of dynamical transformations among F_3^{+-} , F_3^- , and F_4 -centers, and most probably also the other remaining centers are involved in them more or less directly.

2.3. Association of glows peaks to color centers. The question as to whether or not GPs in LiF crystals are directly connected with some particular CCs was still open until recently. Establishing an answer to this question has been also a motivating factor of the present investigation. Without going in too much details, which has been done elsewhere [4–7], by looking carefully at the TL curves of Fig. 1, and by keeping in mind the coloration procedures of the samples as reported in Table 1, the following observations and deductions have been made.

Samples *B* and *D*.

1) Sample *B* lacks any TL below 200°C, while sample *D* has the maximum integral TL in the same temperature interval.

2) Sample *B* has been treated in order to have less F_3^+ -centers, while sample *D* has been treated to have more F_3^+ -centers.

3) Measured concentrations of F_3^+ -centers in Table 2 agrees with the previous expectations.

4) Annealing measurements in Fig. 3 show that F_3^+ centers start to decrease quickly at 200°C.

TL near 200°C has been previously associated to F_3^+ and Z_2 defects [20]. Later on, following the previous arguments, the GP at 164°C has been definitively associated with F_3^+ -centers [4,5].

Samples *B* and *C*.

1) Sample *B* lacks any TL below 200°C, while sample *C* has two notable peaks around 200°C, and a pronounced shoulder at 164°C.

2) Sample *B* has been treated in order to have less F_3^+ -centers, while sample *C* has been treated to have less aggregated CCs.

3) Measured concentrations of CCs in Table 2 show that the ratio F_3/F_4 increases by more than one order of magnitude when moving from sample *B* to *C*.

4) Annealing measurements in Fig. 3 show that F_3 -centers start to decrease quickly at 200°C, soon after F_3^+ -centers, when temperature increases.

Following the previous arguments, the GP at 193°C has been associated with the F_3 -centers [6]. By using the same methodology, also the peak at 228°C has been associated to F_3 -centers.

Samples *A* and *B*.

1) Sample *B* lacks any TL below 200°C and shows a pronounced peak at 263°C, which is present also in sample *A*, but here broadened by the persistence of the three previous peaks at 164, 193, and 228°C.

2) The thermal treatment applied to sample *B* has almost isolated this peak. The rest of the TL curve above 250°C is similar in both samples.

3) Measured concentrations of CCs in Table 2 show that F_2 centers predominate in *A* and *B* samples.

4) Annealing measurements in Fig. 3 show that only F - and F_2 -centers are still stable between 200 and 300°C.

By excluding F -centers from consideration since they are still thermally stable above 300°C, the intense GP at 263°C has been associated with the decay of F_2 -centers. F_4 -centers may also contribute, because the transmission spectrum of sample *B* indicates an enhanced concentration of F_4 -centers compared to sample *A*. Annealing experiments show that the F_4 bands initially grow and then decay in the temperature range from about 200 to 400°C which contains the GP under discussion. Nevertheless the association of F_2 -centers with the GP at 263°C has been preferred because of their larger concentration [7].

So, by comparing the GPs from RT to 500°C of four nominally pure LiF crystals colored with gamma rays and treated differently, it has been possible to establish the following links:

- F_3^+ -centers and the GP at 164°C;
- F_3 -centers and two GPs at 193 and 228°C;
- F_2 -centers and the GP at 263°C.

The TL curve above 250°C still remains to be analyzed, but the results obtained up to now support the view that a basic requirement for TL to occur in LiF is the presence of F aggregated centers in the crystals. So, the GPs at 286, 308, 332, and 410°C have been assigned tentatively to F -like centers which are known to exist in LiF especially when associated with impurity ions, however low their concentration may be.

3. Analysis of thermoluminescence

3.1. General considerations. The TL spectrum is the graphical representation of light intensity plotted as a function of temperature (or time), and possesses one or more maxima, called GPs, which are associated with various energy level traps [21,22]. TL is directly related to the band structure of solids and particularly to the effects of the impurities and lattice imperfections. These can be described as defect centers or just centers that may occur when ions of either signs move away from their original sites, thus leaving vacant sites, able to interact with free charge carriers and to trap them; alternatively, ions can diffuse in interstitial positions and break locally the ideal lattice symmetry; finally impurity ions can perturb the lattice order, because of their sizes and valences, generally different from their neighbour ones. Moreover, these extrinsic defects can interact with the intrinsic, ones, and eventually either of them can aggregate in more complex configurations. From an atomic standpoint, a defect can be described by means of sign and number of charge carriers it may interact with, and of the eventual existence of excited states. To such center is associated a characteristic energy which may be defined is the amount of energy able, when supplied, to set the trapped charges free, thus destroying the center and restoring a situation of local order.

The band structure of the insulating crystals can be described in terms of valence and conduction bands, parted from each other by a forbidden gap in which the defects are represented as sites localized at different depths, below the conduction band, where free charge carriers of either sign may be trapped. Therefore, the mapping of the emission study can provide a tool to get detailed information of the trap parameters. Among them, a peculiar parameter is the kinetic order b which ranges between 1 and 2. The former value corresponds to a situation where to a charge (electron) is supplied energy to be raised in the conduction band and, consequently, to fall to a center where it undergoes recombination with a hole. The latter value stands for a situation where this phenomenon has the same probability of retrapping and starting again the whole process. Intermediate cases are likely to occur, as well as contributions from non radiative events for which $b = 0$.

The mathematical models based upon these definitions are rather complex and beyond the purpose of the present work which will be limited to a few meaningful formulas only. In the first order kinetics, $b = 1$, the intensity of TL is given by

$$I(T) = ns \exp\left(-\frac{E}{kT}\right) \exp\left[-\frac{s}{\beta} \int_{T_0}^T \exp\left(-\frac{E}{kT'}\right) dT'\right], \quad (1)$$

where n is the number of the trapped charges, E is the trap depth (eV), k — the Boltzmann's constant, T — the absolute temperature (K), s is the frequency factor (s^{-1}) depending on the number of hits of an electron in the trap which can be considered as a potential well, and $\beta = dT/dt$ is the heating rate. This expression can be evaluated by means of numerical integration and it yields a bell shaped curve, i.e. a GP, with a maximum intensity at a characteristic temperature T_M , which satisfies the following equation:

$$\frac{\beta E}{kT_M^2} = s \exp\left(-\frac{E}{kT_M}\right). \quad (2)$$

From these two equations, it is easily found that T_M does not depend on the number of trapped charges, and that the integral light intensity depends on the initial number of trapped charges, which are in turn proportional to the initial irradiation dose, and independent of the heating cycle. The latter property is very important in radiation dosimetry.

The expressions for second order kinetics, mixed order, general order kinetics are similar and are dealt in several references, but they are not treated in this work where only the first order kinetics has been used for evaluating the energy parameters. This choice will be explained later on.

3.2. Fitting procedures and first order kinetics. Eq. (1) can be used to fit with reasonable easiness a single experimental GP by varying the parameters E , β , and T_M , but when there are more than one single GP, and they are not well resolved in temperature, it is almost impossible to apply such direct approach. So, in

order to overcome these huge difficulties, which in our case are easily observed in Fig. 1 where there are at least eight tangled single GPs, it has been resorted to determine firstly the exact number of single GPs and their approximate band parameters.

For this purpose, the experimental data have been simulated with eight „normal distribution curves“, i.e. Gaussian curves which are symmetrical about their maxima. The best fit of this attempt resulted in residuals as big as 5%, and evident gaps at 130 and 380°C. It was clear that eight Gaussian curves were not enough to fit well our experimental TL results and so, by following the previous indications of gaps, we repeated the simulation with ten single Gaussian curves. The ensuing best fit resulted in residuals below 2.5%, and in general the agreement between the synthetic Gaussian spectra and the experimental TL curves was quite good at an accurate visual inspection.

So, by using the previous Gaussian fit, it has been possible to retrieve the values of the temperature of the peak T_M , and the width ω for each one of the ten GPs. However, while the Gaussian approach allowed for a genuine fit of the TL spectrum, it does not deliver any direct information about the parameters associated with the GPs, i.e. E , s , etc., for which Eq. (1) should be used, or better a sum over all the GPs involved. However, the required mathematics is rather complex in the first order kinetics, and it is even more so in higher order kinetics approaches so that, by taking also in account that the present TL measurements are of preliminary nature and other ones will soon follow, it has been decided to limit the calculation efforts to the first order kinetics alone. Indeed, it is much more important firstly to assess the role of the impurities, rather than embarking in lengthy and refining calculations which could influence the final results less than done by the impurities.

An investigation of the scientific literature on the argument has shown the availability of computer programs, which can be used for TL curve simulation, and also software especially designed to simulate many single and superimposed GPs were found [23–25]. In particular, a friendly manual explaining its practical working was available in Ref. [25] which describes a program, GlowFit, for deconvoluting first order kinetics TL curves. It uses a non-linear function describing a single GP to fit experimental data using the least squares Levenberg–Marquardt method. The program is very suitable for the present case because it requires the initial values of the parameters, already in our possession following the previous ten Gaussian fits, and at the end it allows the manual adjustment of the same parameters by using a graphic interface enabling easy intuitive manipulation of GPs. Fig. 4, *a–d* show the final fit of the four TL curves. Every figure reports the experimental data, dots, the GPs, weak full lines, and their sum, heavy full lines, to be compared with the data. The residuals are less than 2%, a figure which can be considered quite satisfactory at moment, even better than the fit with ten Gaussian curves. The latter result is not unexpected, because the single GPs are asymmetric with respect to their maximum, which is

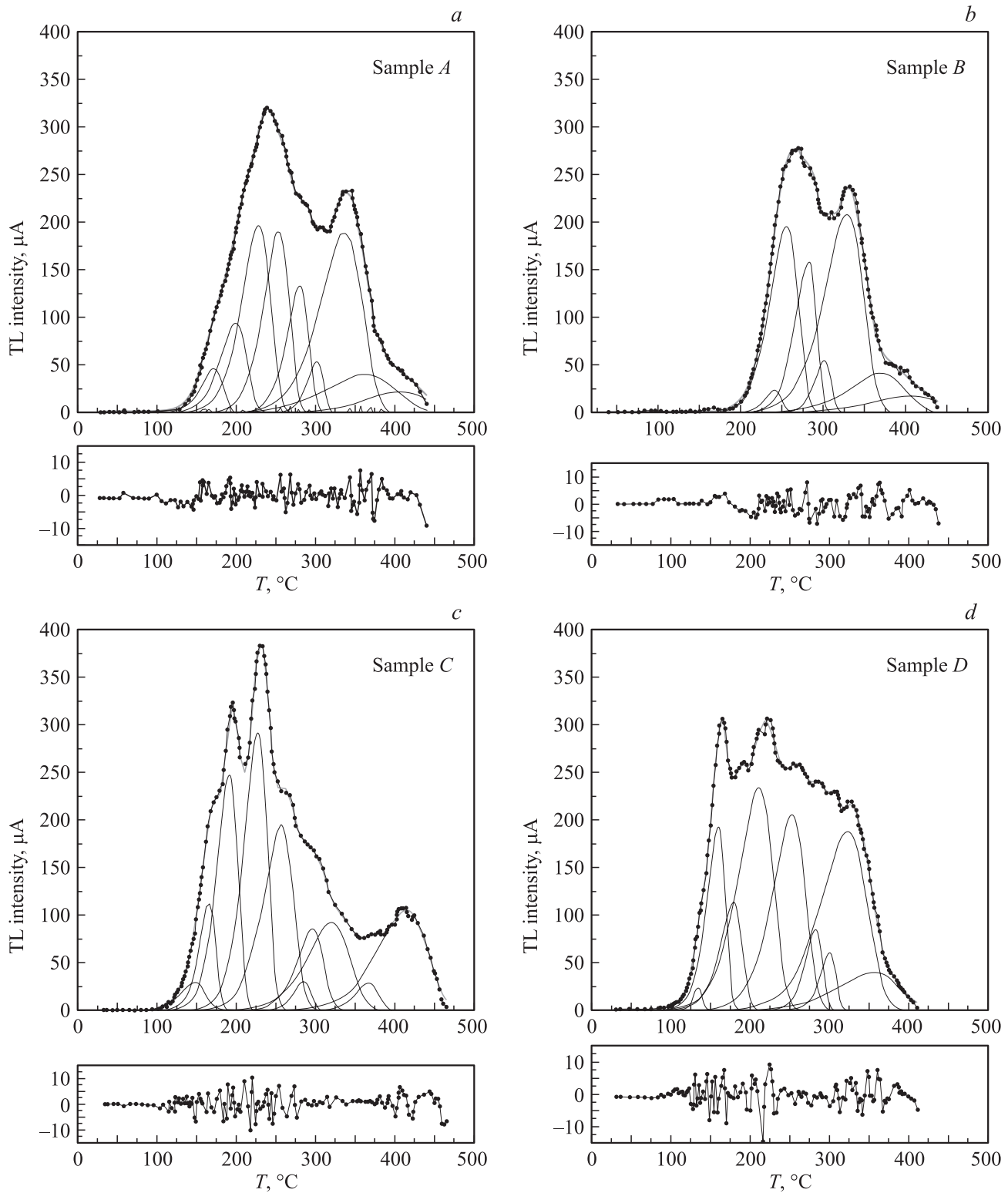


Figure 4. Experimental TL curves of samples A, B, C and D (dots lines), best fit curves (thick lines) with the first order kinetics theory, single GPs (thin lines), and the residuals at bottom. *a* — sample A, *b* — sample B, *c* — sample C, *d* — sample D.

not the case of Gaussian curves. This curve asymmetry fits much better the TL curve especially at the beginning where there is a slow increase of the TL signal, completely out of reach from a Gaussian curve.

4. Discussion and conclusions

From the previous best fit obtained by using the first order kinetics approach it is possible to obtain the values

of T_M and E , while the value of s can be calculated with Eq. (2), where all the other parameters are known. Another important parameter, the width of the GPs, is not given directly by the fit, and in the present case it should be taken into account that the actual GPs are asymmetric with respect to T_M , differently from the previous simulation with Gaussian curves. So, in order to have a qualitative parameter to be used for discussion, it has been resorted to an artificially defined width ω_a such that $\omega_a = A/I_M$, where A and I_M are the area of the GP and the intensity of its maximum, respectively. Because the last two parameters are delivered automatically by the fit program, the values of ω_a are easily calculated. Finally, the values of T_M , E , ω_a , and s are reported in Table 3, together with the already accomplished association of GPs to CCs.

The values of T_M reported in Table 3 can be compared with the same parameters reported in chapter 2.2. By excluding Gps 1 and 9, not retrieved visually in Fig. 1, the comparison is good enough, differences well below 10°C , if one considers the experimental errors and the fit approximations. On the contrary, the widths of the GPs cannot be compared in a quantitative way because of the different definition between ω and ω_a . Anyway, there appear disturbing values of ω_a and s which should be considered more closely, and for that they have been reported in bold in Table 3. Indeed, the temperature width ω_a should not be as big as in the case of GPs 8–10, and s cannot be bigger than the lattice vibration frequency in LiF, $1.26 \cdot 10^{14} \text{ s}^{-1}$, as it is the case of GPs 1, 6, 7 and to a lesser extent GP 2.

It should be remembered that the trap energy depth, the maximum temperature, and the width of the GP are related among them by the following relation:

$$E \cong \frac{kT_M^2}{\omega} \quad (3)$$

for which the energy depth increases with the square of the maximum temperature and decreases with the width of the GP. In general, it is expected that the GPs at higher temperatures correspond to more deep traps, which here is not the case for the GPs 8–10. The observed decrease of the energy in the latter cases is clearly due to the increase of the width, which is so looking suspicious. Indeed, other GPs could exist at temperatures higher than 260°C , resulting to narrower widths and so higher energy depths.

At a better look, the previous conflicting data belong mainly to the first GP at 142°C , not yet associated to any CC, and to TL curve above 260°C , where several GPs are overlapping each other, and are associated to F -like centers related to different impurity ions, of which we do not know the numbers.

So, especially for temperatures above 250 – 300°C , there are not enough experimental data to determine with a reasonable certainty the number of traps involved, which can be more numerous than the ones discovered here. Moreover, it is necessary to remember that in the present work nominally pure LiF crystals have been used, which

Table 3. The values of T_M and E as derived by fitting the experimental TL curves with the first order kinetics approach for ten GPs

Glow curve	T_M , $^\circ\text{C}$	E , eV	ω_a , $^\circ\text{C}$	s , s^{-1}	CCs
1	142	1.81	14	$2.7 \cdot 10^{20}$	—
2	162	1.45	15	$1.3 \cdot 10^{15}$	F_3^+
3	190	1.32	18	$4.2 \cdot 10^{12}$	F_3
4	224	1.23	23	$4.4 \cdot 10^{10}$	F_3
5	253	1.30	24	$4.8 \cdot 10^{13}$	F_2
6	281	2.16	16	$8.9 \cdot 10^{17}$	F -like
7	300	2.51	17	$2.7 \cdot 10^{20}$	F -like
8	328	1.16	32	$5.0 \cdot 10^7$	F -like
9	363	1.20	42	$2.7 \cdot 10^7$	—
10	412	1.21	33	$6.0 \cdot 10^6$	F -like

Note. From the previous values and those relative to the intensities and areas, also the artificially defined width ω_a , and the frequency factor s have been calculated. Finally, also the association of GPs to CCs have been reported in the last column for completeness. A few values of ω_a and s have been reported in bold because there are somehow unusual with respect to the other ones. See text for details.

in any case contain impurities in ppm amounts, enough to generate complex CCs related to F -centers, as usually known and shown recently in detail [26,27]. Moreover, a comparison with the known energy diagrams of the various CCs, which up to now have been associated with the GPs, does not seem useful at moment. Indeed, apart the first few GPs below 260°C , the other ones are associated to mostly unknown CCs and, anyway, it is necessary to take also into account that the interpretation of the experimentally observed TL spectra in general is still a matter of lively discussion [28].

Anyway, by comparing the GPs from RT to 500°C of four nominally pure LiF crystals, colored with gamma rays and treated thermally and optically, it has been possible to establish a link between F_3^+ , F_3 , F_2 , and F -like CCs, and four resolved and six unresolved GPs.

The analysis of the relatively complex TL spectra has been greatly simplified by using a visual method and a simple fitting with ten Gaussian curves, which proved to be a useful method to disentangle complex situations in TL.

The ensuing first order kinetics approach has furnished the much searched TL parameters, although a few values of the temperature width and frequency factor are not in agreement with the expected behavior, and hint at more GPs especially above 260°C .

At moment, higher order kinetics analyses are not convenient to be pursued, because most probably the previous disagreements originate mostly from ion impurities, and so it would only produce new values of the parameters without any physical meaning. This is also the main reason why the present analysis was limited only to the first order kinetics.

In conclusion, although we have for the first time derived the TL parameters of nominally pure LiF crystals and associated well defined CCs to some GPs, it appears more safe to postpone a close comparison of the present data with

previous ones, and a detailed discussion of the association of GPs to CCs to later times when more TL spectra will be available. Indeed, other LiF samples are being studied which have been subjected to different irradiation doses and different physical treatments and also, very important, containing different amount of impurities. So, a full understanding of TL in pure LiF crystals has not yet been obtained, but some facets of it have been disclosed and the search is continuing.

The authors are indebted with A.T. Davidson, A. Kozakiewicz, R.M. Montecchi, and E. Nicolatti for their general involvement in this subject and useful discussions. Many thanks are due to A. Pace and M.A. Vincenti for their invaluable technical support.

References

- [1] J.J. Hill, P. Schwed. *J. Chem. Phys.* **23**, 652 (1955).
- [2] M.R. Mayhugh. *J. Appl. Phys.* **41**, 4776 (1970).
- [3] F. Sagastibelza, J.L. Alvarez Rivas. *J. Phys. C: Solid State Phys.* **14**, 1873 (1981).
- [4] G. Baldacchini, A.T. Davidson, V.S. Kalinov, A.G. Kozakiewicz, R.M. Montecchi, A.P. Voitovich. *J. Lumin.* **102–103**, 77 (2003).
- [5] G. Baldacchini, A.T. Davidson, V.S. Kalinov, A.G. Kozakiewicz, T. Marolo, M. Montecchi, R.M. Montecchi, E. Nichelatti, A.P. Voitovich. *Opt. Mater.* **24**, 129 (2003).
- [6] G. Baldacchini, A.T. Davidson, V.S. Kalinov, A.G. Kozakiewicz, R.M. Montecchi, E. Nichelatti, A.P. Voitovich. *J. Lumin.* **122–123**, 371 (2007).
- [7] G. Baldacchini, A.T. Davidson, V.S. Kalinov, A.G. Kozakiewicz, R.M. Montecchi, E. Nichelatti, A.P. Voitovich. *Phys. Status Solidi C* **4**, 972 (2007).
- [8] G. Baldacchini. *J. Lumin.* **100**, 333 (2002).
- [9] R.M. Montecchi. In: *Handbook of thin film materials* / Ed. H.S. Nalwa. V. 3. Ferroelectric and dielectric thin films. Academic Press (2002). P. 399.
- [10] N. Miura. In: *Phosphor handbook* / Eds S. Shionoya, W.M. Yen. CRC Press, Boca Raton (1998). P. 521.
- [11] D.B. Fitchen. In: *Physics of color centers* / Ed. W.B. Fowler. Academic Press, N.Y. (1968). P. 293.
- [12] A.P. Voitovich, V.S. Kalinov, S.A. Mikhnov, S.I. Ovseichuk. *J. Sov. Quantum Electron.* **17**, 780 (1987).
- [13] M. Montecchi, R.M. Montecchi, E. Nichelatti, M. Piccinini, F. Somma. *Opt. Quantum Electron.* **36**, 43 (2004).
- [14] A.T. Davidson, A.G. Kozakiewicz, D.J. Wilkinson, J.D. Comins, T.E. Derry. *Nucl. Instrum. Meth. Phys. Res. B* **141**, 523 (1998).
- [15] J.M. Bunch, E. Pearlstein. *Phys. Rev.* **181**, 1290 (1969).
- [16] V. Ausin, J.L. Alvarez Rivas. *J. Phys. C: Solid State Phys.* **5**, 82 (1972).
- [17] C.C. Klick, E.W. Claffy, S.G. Gorbics, F.H. Attix, J.H. Schulman, J.G. Allard. *J. Appl. Phys.* **38**, 3867 (1967).
- [18] J.H. Crawford, Jr. *Adv. Phys.* **17**, 65, 93 (1968).
- [19] G. Baldacchini, T. Marolo, R.M. Montecchi, A. Pace, V.S. Kalinov, A.P. Voitovich. *Annealing of gamma rays colored LiF Crystals*. ENEA Report RT/2004/67/FIS (2004).
- [20] A.T. Davidson, A.G. Kozakiewicz, D.J. Wilkinson, J.D. Comins. *J. Appl. Phys.* **86**, 1410 (1999).
- [21] R. Chen, S.W.S. McKeever. *Theory of thermoluminescence and related phenomena*. World scientific publishing Co., Singapore (1997).
- [22] C. Furetta, P.-S. Weng. *Operational thermoluminescence Dosimetry*. World Scientific Publishing Co., Singapore (1998).
- [23] G. Kitis, J.M. Gomez-Ros, J.W.N. Tuyn. *J. Phys. D: Appl. Phys.* **31**, 2636 (1998).
- [24] K.S. Chung, H.S. Choe, J.I. Lee, J.L. Kim, S.Y. Chang. *Rad. Prot. Dosim.* **115**, 345 (2005).
- [25] M. Puchalska, P. Bilski. *Rad. Meas.* **41**, 659 (2006).
- [26] G. Baldacchini, O. Goncharova, V.S. Kalinov, R.M. Montecchi, E. Nichelatti, A. Vincenti, A.P. Voitovich. *Phys. Status Solidi C* **4**, 744 (2007).
- [27] G. Baldacchini, O. Goncharova, V.S. Kalinov, R.M. Montecchi, A. Vincenti, A.P. Voitovich. *Phys. Status Solidi C* **4**, 1134 (2007).
- [28] S. Basun, G.F. Imbush, D.D. Jia, W.M. Yen. *J. Lumin.* **104**, 283 (2003).